

01,05

Enhancement of magnetocaloric efficiency of Gd spacer between strong ferromagnets

© I.Yu. Pashenkin¹, N.I. Polushkin¹, M.V. Sapozhnikov¹, E.S. Demidov², E.A. Kravtsov^{3,4}, A.A. Fraerman¹

¹Institute for Physics of Microstructures, Russian Academy of Sciences, Nizhny Novgorod, Russia

²Lobachevsky State University, Nizhny Novgorod, Russia

³M.N. Mikheev Institute of Metal Physics, Ural Branch, Russian Academy of Sciences, Yekaterinburg, Russia

⁴Ural Federal University after the first President of Russia B.N. Yeltsin, Yekaterinburg, Russia

E-mail: nip@ipmras.ru

Received April 29, 2022

Revised April 29, 2022

Accepted May 12, 2022

The magnetocaloric properties of a thin spacer of gadolinium (Gd) between layers of „strong“ ferromagnets (relatively high Curie temperatures) are studied experimentally. It is found that, at room temperatures, the magnetocaloric efficiency $\Delta S/\Delta H$ (ΔS is the isothermal magnetic entropy change and ΔH is the range of applied magnetic fields) of Gd spacer of thickness of 3 nm is up to two orders in magnitude higher than this value in an individual thicker (30 nm) Gd layer. This opens up opportunities for using the magnetocaloric effect in micro(nano)electronics and biomedicine using relatively weak magnetic fields $H < 1$ kOe. The observed increase in the magnetocaloric efficiency is explained by the influence of direct exchange coupling between Gd spacer and its surroundings, which changes the distribution of magnetization in the spacer and, ultimately, its magnetocaloric potential.

Keywords: magnetocaloric effect, magnetic heterostructures, exchange coupling at interfaces, Curie temperature.

DOI: 10.21883/PSS.2022.10.54215.30HH

1. Introduction

Usually a sufficiently large (up to $\Delta T \sim 10$ degrees Kelvin) magnetocaloric effect (MCE) is achieved by applying a magnetic field H of several tens of kilooersteds to the refrigerant at temperatures T close to the Curie temperature T_C [1,2]. However, such strong fields can only be produced using bulky magnets, which are undesirable for magnetic cooling [3,4]. This especially includes possibilities of using MCE in micro(nano)electronic devices, as well as micro(nano)electromechanical systems [4–6] and biomedicine [7]. Such applications require microscopically small volume cooling/heating, which can be realized with a thin-film magnetocaloric material. In our work we explore if possible to obtain the MCE in a thin magnetic layer exposed by a relatively weak $H < 1$ kOe. The system studied is a few nanometers thick spacer of refrigerant sandwiched by ferromagnetic layers whose Curie temperatures are substantially higher („strong“ ferromagnets) than T_C of the spacer. In the context of this study, an important parameter is the exchange coupling strength acting at the interfaces between the refrigerant and its „strongly“ ferromagnetic surroundings [8–14]. A magnetic field not bigger than a few hundred oersted applied to such a system induces switching of magnetization in a softer surrounding. This reconfiguration leads to the change in magnetic entropy of

the spacer owing to redistribution of magnetization in it. The magnetic entropy change (magnetocaloric potential), ΔS , relates to the temperature change, that is, $\Delta T = (T_C/c_V)\Delta S$, where c_V is specific heat capacity of the refrigerant [1]. Theoretically, it was shown [8–10] that the MCE in such a system can reach values up to several degrees Kelvin at $H < 1$ kOe.

This article presents the results of experimental studies of the MCE in a layer of gadolinium (Gd), which is in direct contact across interfaces with layers of magnetically soft (Fe/FeCoB) and magnetically hard (Fe/CoSm) materials. Gd is one of the well studied magnetocaloric materials to be used for magnetic cooling in both the bulk [1,2] and thin-film [15,16] forms. Obtained values of the magnetocaloric efficiency $\Delta S/\Delta H$ (ΔH is a range of H applied) were compared to those for a separate Gd layer [15].

2. Experiment

The exact composition of the system under study is substrate(glass)/TaO/F1/Gd/F2/TaO, where F1 is bilayer of strong ferromagnet (2 nm)Fe₄₀Co₄₀B₂₀/(1 nm)Fe, while F2 is a layer of (2 nm)Fe with 30 nm thick sublayer of Co₇₅Sm₂₅ (Fig. 1). In F1 the layer of Fe was deposited to be adjacent to Gd, in order to provide strong exchange coupling between Fe and Gd [17]. The samples were

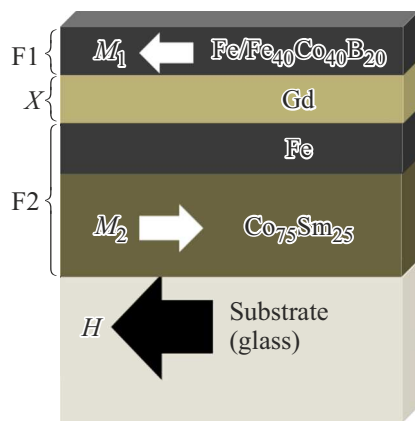


Figure 1. Schematic representation of F1/Gd/F2 system under study. The antiferromagnetic configuration of the magnetizations M_1 and M_2 of strong ferromagnets F1 and F2 is shown. Reorientation of M_1 occurs in a magnetic field H that exceeds the switching field of layer F1, but does not exceed the switching field of F2.

prepared by magnetron sputtering in an AJA 2200 multi-chamber system at base pressure of $5.0 \cdot 10^{-8}$ Torr. Gd thickness was varied from 2.5 to 5.0 nm. Layers of TaO (5 nm in thickness) were deposited to prevent oxidation and chemical interaction of the magnetic layers (especially, Gd) with the substrate.

The magnetic and magnetocaloric properties of the prepared samples were studied by detecting the magnetic moment m of the sample using the vibration magnetometer by Lake Shore Cryotronics, Inc. in a field H applied in the sample plane along the easy magnetization axis at temperatures in the range of 170–320 K with a step of 30 K. From the dependences $m(H)$ obtained, the magnetocaloric potential was determined using the Maxwell's thermodynamic relation.

3. Results

The temperature range in which the dependences $m(H)$ were measured was chosen taking into account the fact that the Curie temperature of a very thin (< 10 nm) Gd layer is significantly lower than that of the bulk [15,18] and strongly depends on layer thickness [19,20]. It is expected that the switching fields H_1 and H_2 in the soft F1 and hard F2 layers, respectively, should be so different that magnetization reversal of the system as a whole would be two-stage. Within a field range of $H_1 < H < H_2$, because of exchange coupling to F1 and F2 across the interfaces, the occurring redistribution of magnetization in the spacer affects the magnetic entropy in it [8–10].

Figure 2 shows obtained dependences of the magnetic moment m of the sample on the magnetic field H applied to F1/Gd/F2 samples with Gd thickness of 5 and 3 nm. The presented m -versus- H dependences demonstrate a two-step-like and symmetric with respect to $H = 0$ switching of magnetization. In both plots of Fig. 2, *a, b*, the arrows indicate the first stage, i.e. switching of F1. As can be seen, the switching of magnetization in the soft F1 layer is well distinguishable from that in the magnetically hard F2 layer, so that one can determine the change in magnetic entropy upon switching of F1. In particular, in the sample with 5-nm-thick spacer, switching of F1 occurs at $H \sim 100$ Oe over the entire temperature range under study, while F2 toggles at H reaching values ~ 1 kOe and higher (Fig. 2, *a*). It is also seen that switching of F1 is sensitive to temperature variation. This is more pronounced in the sample with thinner (3 nm) spacer (Fig. 2, *b*). Obviously, the stronger this temperature sensitivity, the higher the magnetocaloric potential of the system under study.

In these experiments, we focused mostly on the low-field stage of magnetization reversal, that is, switching of F1, which provides the MCE in the studied systems.

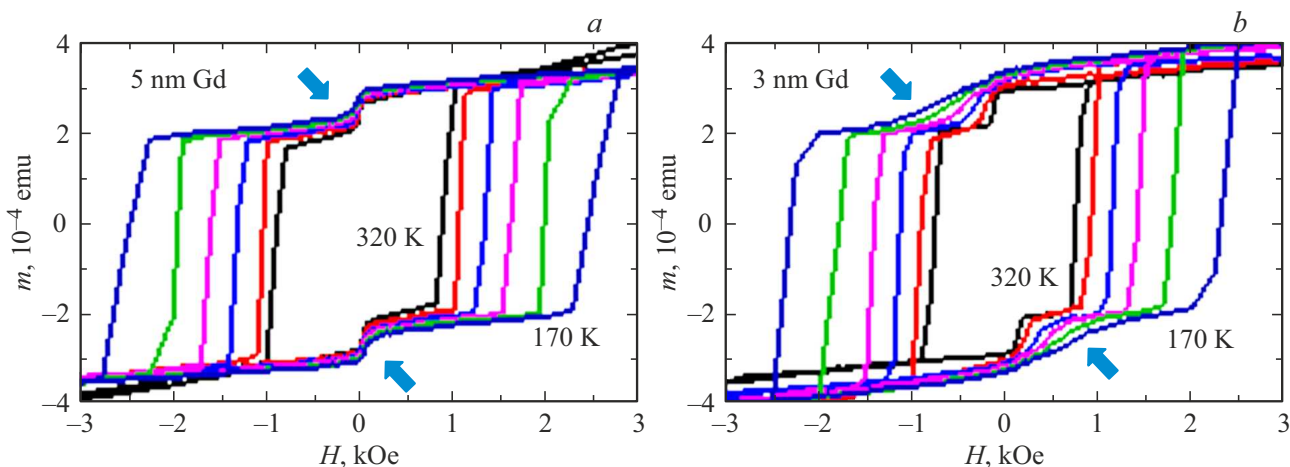


Figure 2. Hysteresis loops of F1/Gd/F2 samples with Gd spacer thickness of 5 (*a*) and 3 (*b*) nm in the temperature range from 320 to 170 K. The arrows indicate the first (low-field) stage of the magnetization curve, namely switching of F1. Switching of F2 occurs upon applying a bigger H .

Figure 3, *a, b* shows fragments of hysteresis loops in units of $M = m/V_{F1}$ (V_{F1} is volume occupied by F1), which indicate switching of magnetization in the soft F1 layer. A characteristic feature of the obtained magnetization curves is the slope breaks indicated by intersections with dashed horizontal lines in Fig. 3, *a, b*. This plotting enables us to identify the locations where reorientation of the vector M_1 basically occurs, so the total change in magnetization is doubled saturation magnetization in F1 ($2M_{1s}$).

A more detailed definition of the field interval $\Delta H = H_u - H_l$, in which switching of F1 occurs, is shown in Fig. 3, *c*, while Fig. 3, *d* illustrates the dependence of ΔH on T for samples with Gd thickness of 5 and 3 nm. In the observed magnetization curves, attention is drawn to the fact that there are strong changes in the magnetization even before switching of H after its saturation in a large applied field. This feature can be explained by the reorientation of magnetic moments in Gd, which prefer to be oriented antiparallel to the magnetization direction in F1 and F2 [17] in a sufficiently weak field. This behavior is schematically illustrated in Fig. 4.

It is also striking that there is a strong retardation of magnetization switching in F1 with thinning the spacer. For example, if Gd thickness is 5 nm, magnetization in F1 toggles at $H \sim 10$ Oe, while this switching starts only at $H > 100$ Oe in the sample with 3-nm-thick Gd spacer. This fact witnesses the discontinuity of the Gd spacer with thickness of 3 nm, so that direct exchange appears between F1 and F2 through the spacer.

The magnetocaloric potential of the F1/Gd/F2 samples under study was determined from the $M-H$ magnetization curves in the ΔH field range from H_l to H_u , taking into account the Maxwell's thermodynamic relation

$$\Delta S = \int_{H_l}^{H_u} \frac{\partial M(H, T)}{\partial T} dH. \quad (1)$$

H_l and H_u were defined respectively as the first and second inflections of the magnetization curve (Fig. 3, *a-c*). With a further increase of H , initially gradual and then steep (after the third inflection) switching of F2 takes place. The value of ΔS , which depends on T , was determined approximately by calculating the values of $[M(H, T_i) - M(H, T_{i+1})]/\Delta T$, where $i = 1, 2, 3, 4, 5$ and T_i are temperatures from $T_1 = 320$ K to $T_6 = 170$ K with the step of $\Delta T = T_i - T_{i+1} = 30$ K, and then integrating the calculation result over the field interval $\Delta H = H_u - H_l$ corresponding to T_i . At each temperature interval $T_i - T_{i+1}$ the obtained ΔS was assigned to the average temperature value in this interval, $(T_i + T_{i+1})/2$.

Figure 5 illustrates the obtained temperature dependence of the magnetocaloric potential ΔS and the magnetocaloric efficiency $\Delta S/\Delta H$ in the samples under study. The values of ΔS are shown for samples with Gd spacer thicknesses of 5 and 3 nm, while $\Delta S/\Delta H$ are given for samples with Gd thicknesses of 3 nm only and are compared with this

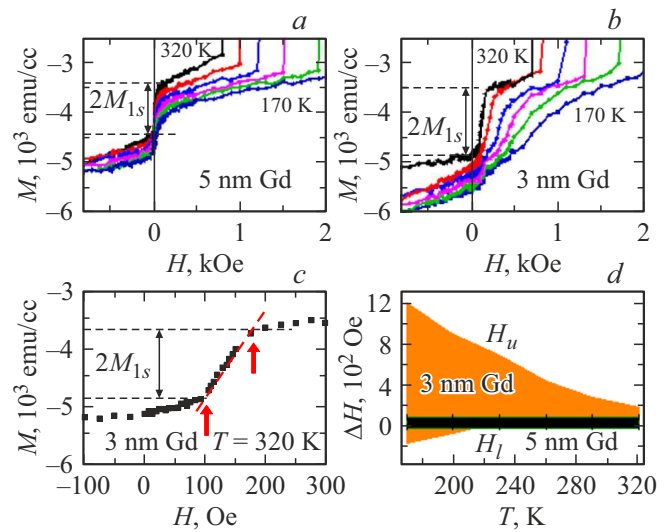


Figure 3. (*a, b*) Fragments of magnetization curves in magnetization units of $M = m/V_{F1}$ (V_{F1} is volume of F1) of F1/Gd/F2 samples with Gd spacer thicknesses of 5 and 3 nm in the temperature range from 320 to 170 K. (*c*) An example for determining the field interval $\Delta H = H_u - H_l$, in which magnetization in F2 toggles. (*d*) ΔH as a function T for samples with Gd thicknesses of 5 and 3 nm.

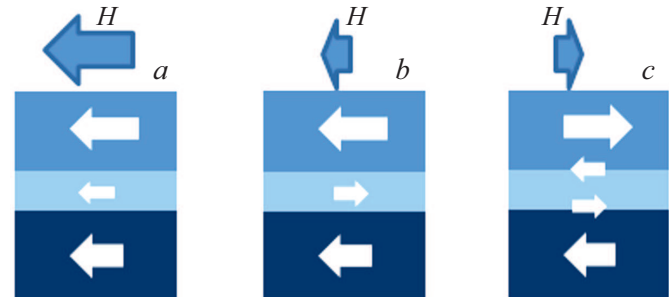


Figure 4. Schematic view of magnetization configurations in the F1/Gd/F2 structure depending on the magnitude and direction of H : (*a*) The applied field $H < 0$ is so strong that Gd spacer is completely magnetized in the direction of magnetizations in F1 and F2. (*b*) The value of $H < 0$ decreases so that the direction of magnetization in Gd is reversed. (*c*) Reorientation of magnetization in the magnetically soft layer F1 (upper layer) upon switching the direction (sign) of H causes a redistribution of magnetization in the spacer.

magnitude for a separate thicker (30 nm) Gd layer [15]. As can be seen, ΔS strongly decreases with thickening the spacer up to 5 nm (Fig. 5, *a*). It is also noteworthy that the magnetocaloric efficiency $\Delta S/\Delta H$ in the F1/(3 nm)Gd/F2 sample significantly exceeds this value in a separate Gd layer. Moreover, in the temperature range near room temperature, which is important for possible applications of the MCE, this excess reaches up to two orders in magnitude. Thus, under the condition of system organization for the multicyclic process of magnetic cooling

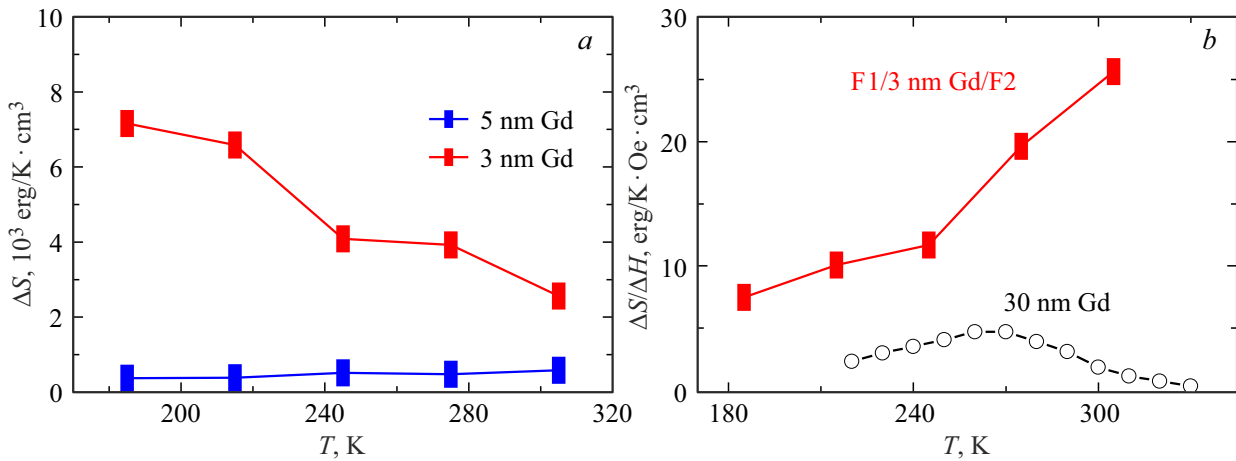


Figure 5. Temperature dependences of the magnetocaloric potential ΔS (a) and efficiency $\Delta S/\Delta H$ (b) in F1/Gd/F2 samples. The values of ΔS are shown for samples with 5 and 3 nm Gd thicknesses, while $\Delta S/\Delta H$ are given for the sample with 3 nm thick Gd and are compared with this magnitude for a separate thicker (30 nm) Gd layer [15].

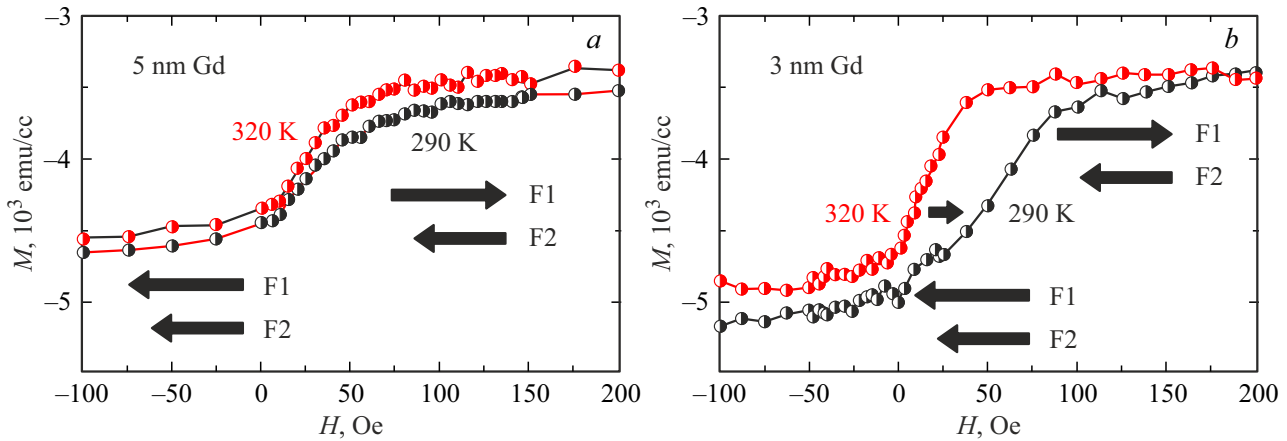


Figure 6. Switching of F1 at $T = 320$ K and $T = 290$ K in the samples with Gd thickness of 5 (a) and 3 (b) nm. In the temperature range of 320–290 K, the magnetocaloric efficiency is highest due to a relatively narrow range of fields ΔH (Fig. 3, a), in which switching of F1 occurs. Retardation of magnetization switching in F1 with decreasing temperature qualitatively characterizes the system's ability to MCE. The longer the delay in the start of switching the higher the magnetocaloric potential of the system.

in weak magnetic fields $H \sim 100$ Oe, it would be attractive to use the F1/Gd/F2 structure.

4. Discussion

The observed increase in the magnetocaloric efficiency $\Delta S/\Delta H$ in studied F1/Gd/F2 samples as compared to a separate Gd layer (Fig. 5) can be qualitatively explained in terms of interlayer coupling between „strong“ ferromagnets F1 and F2 through a „weakly“ ferromagnetic spacer of Gd. When the system is magnetized by a sufficiently strong H , magnetizations of all the layers are oriented in the same direction (Fig. 4, a), so that the magnetic entropy of Gd spacer gets its minimum. It can be assumed that the entropy remains still small when Gd magnetization just toggles with decreasing H (Fig. 4, b), which is due to antiferromagnetic coupling of Gd to F1 and F2 [17,20]. However, if

H changes its direction and becomes sufficiently strong to induce switching of F1, Gd magnetization becomes inhomogeneous over the spacer thickness in such a manner that Gd magnetic moments near the interfaces with F1 and F2 become oriented antiparallel to the F1 and F2 magnetizations (Fig. 4, c). At T close to T_C , the entropy of an ferromagnet can be increased in a non-uniform state of magnetization in it [8–10].

Within the phenomenological model of interlayer exchange [21] the free energy of F1/Gd/F2 system is written as

$$F = -J(T)M_1M_2 \cos \vartheta + M_1H \cos \vartheta, \quad (2)$$

where J is the temperature-dependent T interlayer exchange constant between F1 and F2 through the spacer, and ϑ is the angle between the magnetizations M_1 and M_2 . Depending on the value and sign of H , the equilibrium state is realized in the system either at $\vartheta = 0$ (Fig. 4, a, b) or at $\vartheta = \pi$

(Fig. 4, *c*). Taking into account the relation $S = -\partial F/\partial T$, the magnetocaloric potential is [12,13]:

$$\Delta S = 2 \frac{dJ}{dT} M_1 M_2, \quad (3)$$

where the meaning of JM_2 is the effective exchange field acting on F1 from the magnetically hard F2. The magnitude of this field can be determined experimentally as a magnetic field H in which the magnetization M_1 changes its direction for opposite one. It is seen (Fig. 3, *a, b*) that, in a real system, the switching is smearing over a broad range of H . So the magnetocaloric potential ΔS relates to the increase in the effective switching field of F1 with lowering T (Fig. 6). The value of this field can be defined as $\Delta H/2$ (Fig. 3, *d*). It is interesting that, with temperature variation, the switching field in the sample with 3 nm thick Gd is much larger than that with 5 nm thick Gd. This qualitatively reflects strengthening the MCE with thinning the spacer. To quantify the effect of spacer thickness, one may compute ΔS using the Maxwell's relation (1). The results of such computation are illustrated in Fig. 5, *a*.

5. Conclusion

The magnetocaloric properties of ultrathin Gd layers, which on both sides are in direct contact with „strong“ ferromagnets F1 and F2 (with comparatively high Curie temperatures), are experimentally investigated. The goal of this study was to verify the hypothesis that the magnetocaloric efficiency of Gd spacer in an F1/Gd/F2 system can be increased due to exchange coupling at the interfaces, so that the built-in magnetic field in the system of the exchange nature would play the role of external magnetic field. It is shown that, at room temperatures, the magnetocaloric potential of the Gd spacer with thickness of 3 nm in external magnetic field $H \sim 100$ Oe substantially (up to two orders of magnitude) exceeds this value for a separate thicker (30 nm) Gd layer. This opens the potential for applying the magnetocaloric effect in micro- and nanoelectronic devices, micro- and nanoelectromechanical systems, and also in biomedicine.

Funding

This study was supported by the RFBR (grant No. 20-02-00356) and by the Ministry of Science and Higher Education of the Russian Federation (No. 0030-2021-0021 and 0030-2022-0006).

Conflict of interest

The authors declare that they have no conflict of interest.

References

- [1] A.M. Tishin, Y.I. Spichkin. The magnetocaloric effect and its application. IOP Publishing Ltd., Bristol and Philadelphia (2003). 475 p.
- [2] K.A. Gschneidner Jr, V.K. Pecharsky, A.O. Tsokol. Rep. Prog. Phys. **68**, 1479 (2005).
- [3] T. Mukherjee, S. Sahoo, R. Skomski, D.J. Sellmyer, Ch. Binck. Phys. Rev. B **79**, 144406 (2009).
- [4] M.R. Dudek, K.K. Dudek, W. Wolak, K.W. Wojciechowski, J.N. Grima. Sci. Rep. **9**, 17607 (2019).
- [5] M.H. Phan, S. Chandra, N.S. Bingham, H. Srikanth, C.L. Zhang, S.W. Cheong, T.D. Hoang, H.D. Chinh. Appl. Phys. Lett. **97**, 242506 (2010).
- [6] P. Lampen-Kelley, R. Madhogaria, N.S. Bingham, M.H. Phan, P.M.S. Monteiro, N.-J. Steinke, A. Ionescu, C.H.W. Barnes, H. Srikanth. Phys. Rev. Mater. **5**, 094404 (2021).
- [7] A.M. Tishin, Y.I. Spichkin, V.I. Zverev, P.W. Egolf. Int. J. Refrig. **68**, 177 (2016).
- [8] A.A. Fraerman and I.A. Shereshevskii, JETP Letters **101**, 9, 618 (2015).
- [9] A.A. Fraerman. JETP Letters, **113**, 5, 356 (2021).
- [10] M.A. Kuznetsov, A.B. Drovosekov, A.A. Fraerman. Journal of Experimental and Theoretical Physics **132**, 1, 79 (2021).
- [11] E.V. Skorokhodov, E.S. Demidov, S.N. Vdovichev, A.A. Fraerman. Journal of Experimental and Theoretical Physics **124**, 4, 617 (2017).
- [12] S.N. Vdovichev, N.I. Polushkin, I.D. Rodionov, V.N. Prudnikov, J. Chang, A.A. Fraerman. Phys. Rev. B **98**, 014428 (2018).
- [13] N.I. Polushkin, I.Y. Pashenkin, E. Fadeev, E. Lahderanta, A.A. Fraerman. J. Magn. Magn. Mater. **491**, 165601 (2019).
- [14] M.A. Kuznetsov, I.Y. Pashenkin, N.I. Polushkin, M.V. Sapozhnikov, A.A. Fraerman. J. Appl. Phys. **127**, 18, 183904 (2020).
- [15] C.W. Miller, D.D. Belyea, B.J. Kirby. J. Vac. Sci. Techn. A **32**, 040802 (2014).
- [16] L. Helmich, M. Bartke, N. Teichert, B. Schleicher, S. Fähler, A. Hütten. AIP Adv. **7**, 056429 (2017).
- [17] D. Haskel, G. Srajer, J.C. Lang, J. Pollmann, C.S. Nelson, J.S. Jiang, S.D. Bader. Phys. Rev. Lett. **87**, 20, 207201 (2001).
- [18] A.B. Drovosekov, N.M. Kreines, A.O. Savitsky, E.A. Kravtsov, M.V. Ryabukhina, V.V. Proglyado, V.V. Ustinov. J. Phys.: Condens. Matter **29**, 115802 (2017).
- [19] B. Khodadadi, J.B. Mohammadi, C. Mewes, T. Mewes, M. Manno, C. Leighton, C.W. Miller. Phys. Rev. B **96**, 054436 (2017).
- [20] M. Taborelli, R. Allenspach, G. Boffa, M. Landolt. Phys. Rev. Lett. **56**, 2869 (1986).
- [21] J.F. Cochran, J.R. Dutcher. J. Appl. Phys. **64**, 6092 (1988).